Effects of MHD instabilities on neutral beam current drive

IOP Publishing | International Atomic Energy Agency Nuclear Fusion
Nucl. Fusion **55** (2015) 053018 (9pp) doi:10.1088/0029-5515/55/5/053018

# Effects of MHD instabilities on neutral beam current drive

**M. Podestà, M. Gorelenkova, D.S. Darrow, E.D. Fredrickson, S.P. Gerhardt and R.B. White**

Princeton Plasma Physics Laboratory, Princeton University, Princeton, NJ-08543, USA

E-mail: mpodesta@pppl.gov

Received 16 December 2014, revised 5 March 2015
Accepted for publication 12 March 2015
Published 17 April 2015


**Abstract**

Neutral beam injection (NBI) is one of the primary tools foreseen for heating, current drive (CD) and q-profile control in future fusion reactors such as ITER and a Fusion Nuclear Science Facility. However, fast ions from NBI may also provide the drive for energetic particle-driven instabilities (e.g. Alfvénic modes (AEs)), which in turn redistribute fast ions in both space and energy, thus hampering the control capabilities and overall efficiency of NB-driven current. Based on experiments on the NSTX tokamak (M. Ono *et al* 2000 *Nucl. Fusion* **40** 557), the effects of AEs and other low-frequency magneto-hydrodynamic instabilities on NB-CD efficiency are investigated. A new fast ion transport model, which accounts for particle transport in phase space as required for resonant AE perturbations, is utilized to obtain consistent simulations of NB-CD through the tokamak transport code TRANSP. It is found that instabilities do indeed reduce the NB-driven current density over most of the plasma radius by up to ∼50%. Moreover, the details of the current profile evolution are sensitive to the specific model used to mimic the interaction between NB ions and instabilities. Implications for fast ion transport modeling in integrated tokamak simulations are briefly discussed.

Keywords: tokamak, MHD instabilities, energetic particle transport, neutral beam current drive

(Some figures may appear in colour only in the online journal)

## 1. Introduction and experimental scenario

Neutral beam injection (NBI) is one of the primary tools foreseen to heat and inject torque in future fusion reactors such as ITER and a Fusion Nuclear Science Facility. In addition, tailored deposition of NB fast ions can be used to vary the radial profile of non-inductive current, thus providing a means to act on the safety factor profile. As a drawback, NB fast ions provide the drive for energetic particle-driven plasma instabilities such as Alfvénic (AEs), kink-like and so-called Energetic Particle modes. Those instabilities, in turn, redistribute fast ions in space and energy, thus affecting the control capabilities and overall efficiency of NB-driven current.

NSTX scenarios with unstable toroidicity-induced AEs (TAEs) and low-frequency, kink-like modes are analyzed to investigate magneto-hydrodynamic (MHD) effects on NB-driven current. Figures 1 and 2 summarize the main properties of instabilities for a particular H-mode discharge with toroidal field $B_t \sim 0.5$ T. A number of TAEs with toroidal mode number $n = 1$–6 are destabilized by NB ions. Their mode structure (figure 2(*b*)) is computed through the NOVA code [1, 2] and rescaled to match measurements from a multi-channel reflectometer system [3] at one specific time, $t \approx 270$ ms. The details of the analysis are found in [4, 5]. A lower frequency, kink-like mode also becomes strongly unstable after $t = 320$ ms. Since no direct mode structure measurements are available at this time, its mode structure, which comprises several toroidal harmonics, is here approximated by a simple analytical model [6] with a dominant $(m, n) = (1, 1)$ component plus smaller $n = 2, 3$ harmonics (figure 2(*c*)).

TAE modes manifest as large amplitude (peak $\delta B/B \sim 10^{-3}$), intermittent bursts—or *avalanches*—which cause substantial drops in the measured neutron rate. Neutron drops are indicative of redistribution of fast ions in both radius and energy [4, 5].

In the remainder of the paper, the methodology utilized for the analyses presented herein is described in section 2. The main results on NB-CD modifications by instabilities are then discussed in section 3. Section 4 concludes the paper with a short discussion on the main implications of this work.

## 2. Analysis methods

Quantitative simulations of NB-CD in the presence of MHD instabilities are inherently related to the modeling of the fast ion evolution under the effects of the modes. In this work, the TRANSP code[2] and its modules are the main tools for

[2] For more details on the TRANSP code, please visit the TRANSP webpage at http://w3.pppl.gov/~pshare/help/transp.htm

 

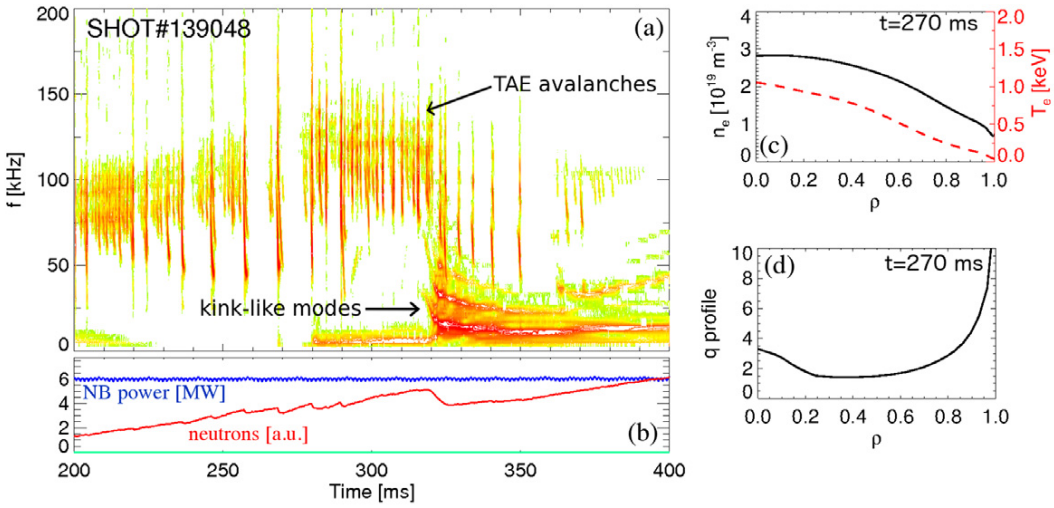


**Figure 1.** Experimental scenario from NSTX #139048. (*a*) Spectrum from Mirnov coils versus time. Red regions indicate larger mode amplitude. (*b*) Traces of NB power and neutron rate. Neutron drops coincide with enhanced mode activity. (*c*) Electron density (solid) and temperature (dashed) profiles versus normalized minor radius, $\rho$, at $t = 270$ ms. (*d*) Profile of the safety factor, $q(\rho)$, at $t = 270$ ms.

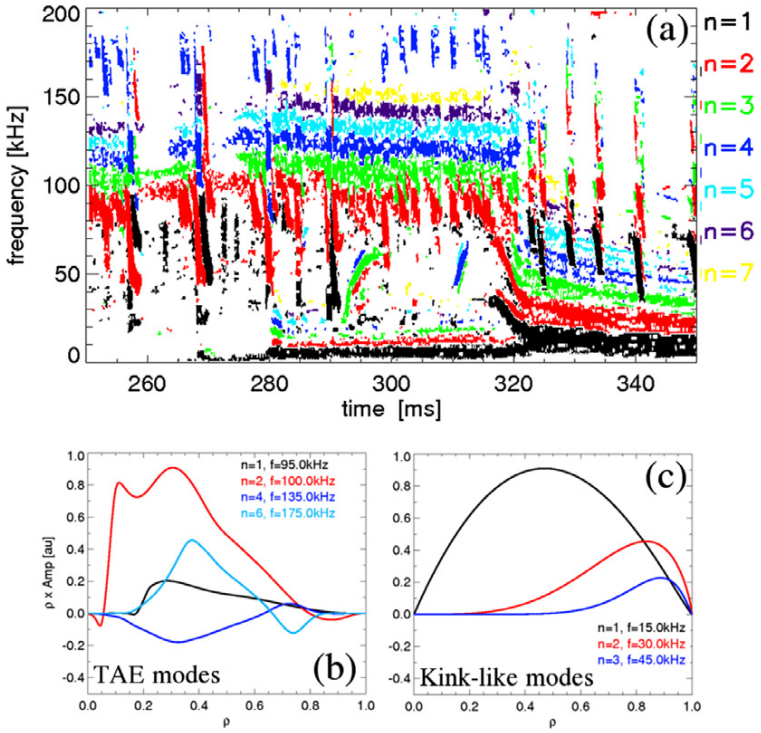


**Figure 2.** (*a*) Mode number spectrum for NSTX discharge #139048, showing dominant TAEs with $n = 1$–6. (*b*) Mode structure from NOVA for the most unstable TAEs in (*a*) around $t \approx 270$ ms. Mode structure is the sum of all poloidal harmonics. (*c*) Mode structure of kink-like modes from a simple model, which mimics a dominant $(n, m) = (1, 1)$ distortion of the equilibrium.

a consistent analysis of NB-driven current which takes into account NB deposition and thermal plasma evolution. Two methods are used. The first method, described in section 2.1, is commonly adopted to model the fast ion evolution when mechanisms other than 'classical' conspire to enhance the fast ion diffusivity. The second method, described in [7] and summarized in section 2.2, has only recently been implemented in the TRANSP code. It is aimed at a more consistent characterization of the effects of instabilities on fast ion evolution.

### 2.1. TRANSP analysis with *effective* fast ion diffusivity

The NUBEAM module [8, 9] implemented in TRANSP models fast ion dynamical evolution in tokamaks based on

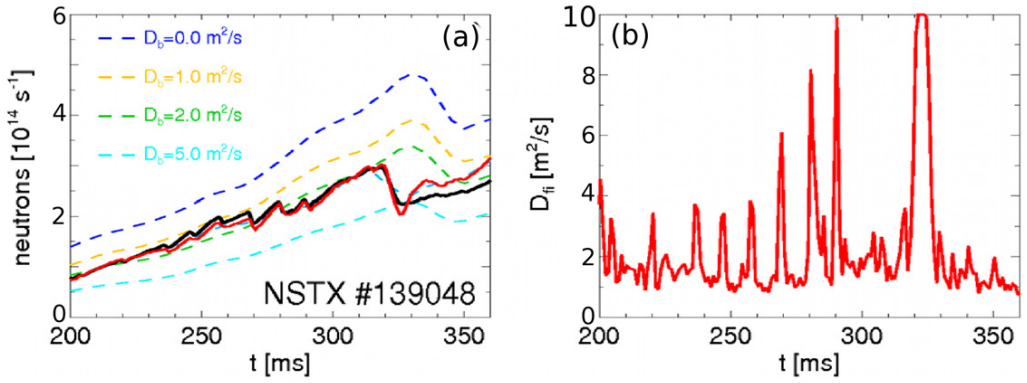


**Figure 3.** TRANSP analysis with fast ion diffusivity $D_{\rm fi}(t)$. (*a*) Measured neutron rate (thick, black) compared to predictions with different levels of diffusivity. Constant values $0 \leqslant D_{\rm fi} \leqslant 5\,{\rm m}^2\,{\rm s}^{-1}$ are used. The thick, red curve shows the predicted neutron rate with a time-varying $D_{\rm fi}$. (*b*) Inferred $D_{\rm fi}(t)$ which gives a satisfactory agreement between predicted and experimental neutron rates in (*a*).

classical physics. In addition, NUBEAM has options to model fast ion transport mechanisms different from classical through ad-hoc diffusivity and convection terms, which result in a radial fast ion flux proportional to the local fast ion density gradient and density. Although these non-classical transport models in NUBEAM do not contain the physics of resonant interaction between instabilities and fast ions, they are widely used and do indeed capture, although empirically, some of the major effects of instabilities on fast ion evolution, see for instance [10–14].

A metric that is commonly used to set the level of additional fast ion diffusivity, $D_{\rm fi}$, is the agreement between measured and simulated quantities such as neutron rate. Typically, $D_{\rm fi}(t)$ is adjusted until a satisfactory agreement is found, see figure 3. A $D_{\rm fi}$ uniform in radius and phase space is used here and in the following. (In principle, more complicated forms for $D_{\rm fi}$ are available, for instance to weight the diffusivity for specific classes of particles—co-passing, trapped, etc—or to impose a non-uniform radial profile. All these choices, however, should be supported by physics considerations on the fast ion interaction with instabilities which are not usually available *a priori*). TRANSP simulations with the adjusted $D_{\rm fi}(t)$ are then used to compute the NB-driven current.

### 2.2. *Kick model for consistent phase space evolution*

The main limitation of TRANSP simulations with an ad-hoc $D_{\rm fi}(t)$ is that wave–particle interaction is treated in a very rough manner, since all fast ions are subject to the same diffusion rate. Even if modifications of fast ion profile or NB-driven current are inferred from the model, uncertainties remain to quantify the relative contribution of each class of instabilities (TAE versus kink-like modes). This can not be properly taken into account by simple modeling with an ad-hoc $D_{\rm fi}(t)$.

Instabilities such as TAEs act on fast ions through specific mechanisms. Consider a particle orbiting in the presence of a single mode with toroidal mode number $n$ and frequency $\omega = 2\pi f$. Based on the Hamiltonian formulation of the Lorentz force equation, a precise relationship exists between mutual variations of energy and toroidal angular momentum ($E$ and $P_\zeta$) [15–17]:

$$\omega P_\zeta - nE = \text{const.} \;\rightarrow\; \Delta P_\zeta/\Delta E = n/\omega \qquad (1)$$

This sets a constraint for the allowed trajectories in the $(E, P_\zeta)$ space, which will be representative of *correlated random walks* rather than a simple, Brownian diffusive motion. Equation (1) applies to the ideal circumstance of a single resonance between an instability and fast ions. In practice, instabilities interact with a fast ion population via several resonances which, depending on the mode amplitude, can be closely spaced in phase space or even overlapping [18]. Rather then relying on an analytical (and rather unpractical) treatment of multiple resonances, a more general approach can be adopted. The main ingredient of the newly developed *kick* model [7] is the probability $p(\Delta E, \Delta P_\zeta | E, P_\zeta, \mu)$ that particles characterized by constant of motions in a phase space *bin* $(P_\zeta, E, \mu)$, experience $E$ and $P_\zeta$ variations of magnitude $\Delta E$ and $\Delta P_\zeta$ ($\mu$ is the magnetic moment). This approach generalizes equation (1) in the presence of multiple resonances between fast ions and a mode (or multiple modes) with amplitude $A_{\rm mode}$. Consistently with the MonteCarlo approach used in NUBEAM, the model aims at reproducing the evolution of an *ensemble* of particles in a statistical sense [7], without pretending to resolve the exact trajectory of each individual particle.

In practice, $p(\Delta E, \Delta P_\zeta)$ can be computed via particle following codes such ORBIT [19] or directly from theory. For this work, the ORBIT code has been modified to compute $p(\Delta E, \Delta P_\zeta)$ and output the probability which is then used in NUBEAM to model the fast ion evolution. Note that the probability is computed in phase space, therefore it represents the average effects of the modes on the entire particle orbit instead of at each point in space. It is assumed that $\mu$ is conserved, which is a reasonable assumption for low-frequency Alfvénic modes with $\omega \ll \omega_{\rm ci}$ ($\omega_{\rm ci}$ being the ion cyclotron resonance frequency), such as TAEs.

An example of the procedure used to compute $p(\Delta E, \Delta P_\zeta)$ is shown in figure 4. Phase space is partitioned into $(P_\zeta, E, \mu)$ bins. For each bin, the kick probability is constructed by sampling $\Delta E$ and $\Delta P_\zeta$ kicks through the ORBIT code. Figures 4(*a*) and (*b*) show examples of the probabilities when either kink-like or multiple TAE modes are used as perturbations in ORBIT. The corresponding root-mean-square (rms) of the $|\Delta E|$ kicks for particles with initial energy of 80 keV is shown in figures 4(*c*) and (*d*) for the entire

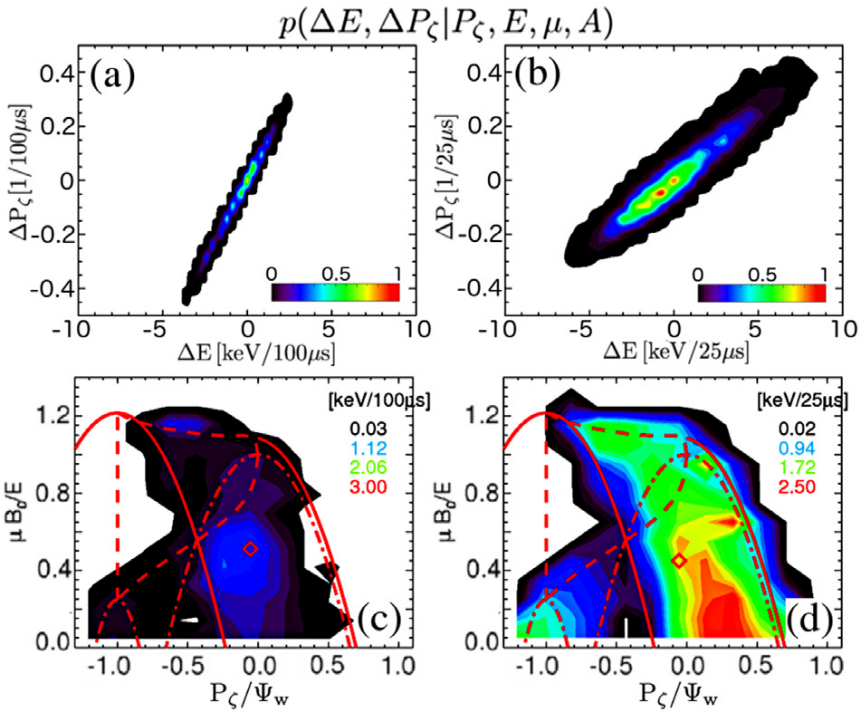


**Figure 4.** Probability $p(\Delta E, \Delta P_\zeta)$ resulting from (*a*) a kink-like mode and (*b*) TAEs for particles with $E = 80$ keV, $P_\zeta \approx 0$ and $\mu B_0/E \approx 0.5$. (*c*)–(*d*) Rms energy kicks for kinks and TAEs for $E \approx 80$ keV.

($P_\zeta$, $\mu$) space. By comparing the two plots, it can be seen that the effects of kink-like and TAE modes differ in terms of both spatial (roughly $\propto P_\zeta$) and pitch ($\mu \propto 1 - p^2$, where the pitch $p = v_{||}/v$ is the ratio of parallel to total velocity).

## 3. NB-CD modifications by MHD

In this section, different models for fast ion transport are used to investigate the effects of instabilities on fast ion dynamics. Results from the two models (ad-hoc $D_{\mathrm{fi}}$ and kick model) are then compared to assess the improvement in simulations when a more realistic approach is used to describe fast ion evolution.

The transient (i.e., over a short time range of the order of the slowing down time) response of the fast ion distribution is first investigated in section 3.1. For this analysis, a *stand-alone* version of the NUBEAM module of TRANSP is used. (The simulation procedure is explained in detail in [7]). Thermal profiles are kept fixed in time, whereas the fast ion distribution is evolved along with NB-driven current profile. Total plasma current and $q(r)$ profile are imposed, based on measurements. Results are indicative of the transient modifications of the fast ion distribution, which can differ depending on the specific model used to mimic the effects of instabilities.

More comprehensive simulations are then performed through the TRANSP code (section 3.2). An example is shown in figure 5 for initial runs with different assumptions on the mode scaling factor. Simulations include the effects of $n = 1, 2$ TAE instabilities during the ramp-up phase, for which a separate set of mode structure and $p(\Delta E, \Delta P_\zeta)$ probability is used. In this case, the focus is on the long time scale evolution of a discharge when different fast ion transport models are used.

### 3.1. Transient analysis

The effects of instabilities are first simulated via the transport code TRANSP by assuming an ad-hoc, radially uniform fast ion diffusivity $D_b(t)$, cf figure 3(*b*). A net redistribution of NB-driven current is observed when instabilities are accounted for, see below. To obtain more accurate results, experiments are interpreted through the new *kick* model. An example of initial simulations for the NSTX scenario described in figures 1–2 is given in figure 6 for a time window in which only TAE modes are observed. The temporal evolution of the total TAE mode amplitude is inferred from the neutron rate variations induced by TAE bursts.

It can be seen that TAE avalanches induce a rapid decrease of fast ion content and NB-driven current. Drops of up to ≈50% are computed for the NB-driven current in the core, and even larger (relative) changes toward the plasma edge. Perturbations of the current profile persist for a considerable fraction of the beam ion slowing down time, which is ∼15–20 ms for this case. The rate of recovery is mainly determined by the NB injection rate. Results obtained from TRANSP with $D_{\mathrm{fi}}(t) \neq 0$ and from the kick model are compared in figures 6(*c*) and (*d*). Drops in the fast ion density are comparable, whereas the ad-hoc $D_{\mathrm{fi}}$ model leads to a smaller redistribution of NB-driven current. This suggests that the $F_{\mathrm{nb}}$ evolution is rather different in the two cases, as expected from the different approaches underlying the two fast ion transport models used in the simulations.

Later in the discharge, a kink-like mode and its harmonics are also destabilized. Results from modeling with the *kick* model are shown in figure 7. TAE mode amplitude is scaled to match the measured level. The normalized kink amplitude

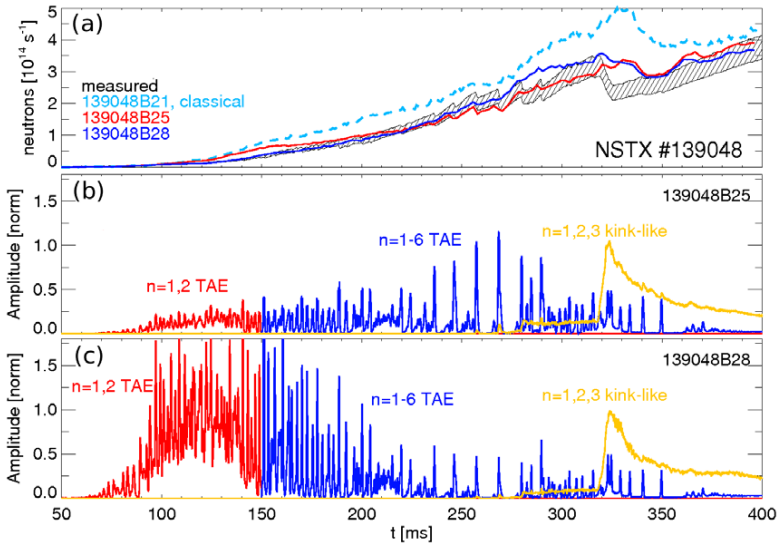


**Figure 5.** (*a*) Comparison of measured neutron rate with TRANSP predictions. TRANSP simulations assume 'classical' fast ion behavior (run #139048B21) and enhanced fast ion transport computed through the 'kick' model (runs #139048B25 and #139048B28) using two different assumptions for the mode amplitude evolution. (*b*) Mode amplitude evolution for run #139048B25, inferred from the Mirnov coils' signal. (*c*) Mode amplitude evolution for run #139048B28, rescaled from that of 139048B25 to obtain a better match with the measured neutron rate.

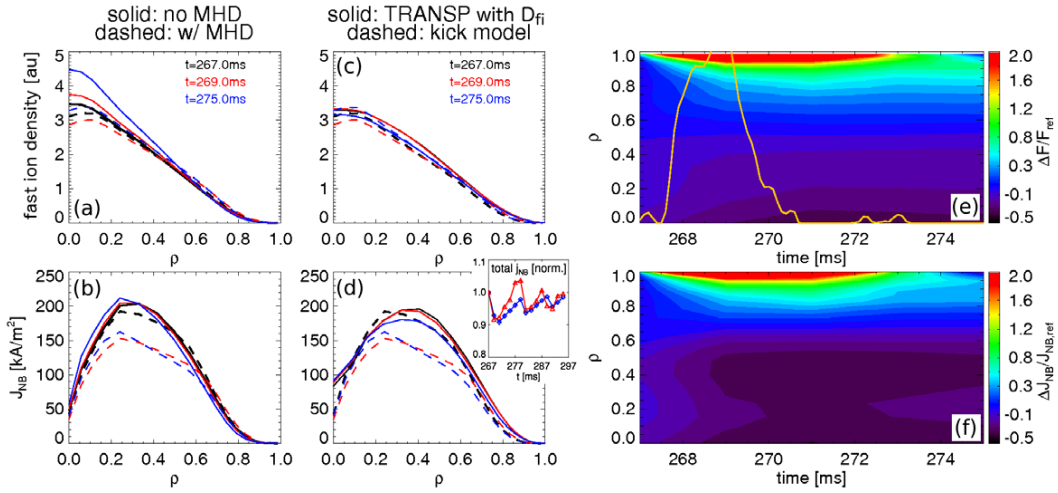


**Figure 6.** Effects of bursting TAEs on fast ion and NB-driven current profiles ($\rho$: normalized radius). (*a*) Fast ion density profile before, just after and 10 ms after a TAE burst, computed through the *kick* model. (*b*) Same as in (*a*) for the NB-driven current profile. Solid (dashed) lines in (*a*) and (*b*) refer to simulations without (with) enhanced transport from TAEs. (*c*)–(*d*) Comparison between fast ion density and $J_{\rm nb}$ computed through *kick* and ad-hoc $D_{\rm fi}$ models. The inset in (*d*) shows the time evolution of the total, normalized NB-driven current obtained with the ad-hoc $D_{\rm fi}$ (red) and with the kick model (blue). (*e*)–(*f*) Relative variation of density and NB-driven current profile versus time, normalized to the no-modes reference case. The solid line in (*e*) shows $A_{\rm mode}(t)$.

from Mirnov coils is then scaled to match the neutron rate. As for the previous example, $p(\Delta E, \Delta P_\zeta)$ is computed through ORBIT [19]. Simulations are performed for TAEs-only, kink-only and TAEs plus kink cases. Because of the different mode structure (figures 2(*b*)and(*c*)) and interaction with fast ions (figures 4(*c*)–(*f*)), the two type of instabilities have a different effect on $J_{\rm nb}$, and especially on its profile. When both instabilities are included, the local drop in $J_{\rm nb}$ exceeds 40% with respect to the no-MHD case, providing an estimate of the rather dramatic effects of instabilities on the overall NB-CD efficiency. Redistribution of fast ions is also significant and mostly affects high energy fast ions, $E \geqslant 50$ keV (figures 7(*e*)–(*g*)).

An interesting result from the examples discussed above is that relative changes in the core fast ion content appear smaller than for the NB-driven current (figures 6(*a*) and (*b*)). Analysis of the inferred phase space modifications (figure 8) indicates that TAEs mainly affect strongly co-passing fast ions with large parallel velocity, which are the most effective in driving parallel current, leaving other portions of the fast ion distribution nearly unperturbed. Clearly, this type of effect cannot be correctly modeled by an ad-hoc diffusion with no selectivity in energy and pitch, whereas it is captured by the new model.

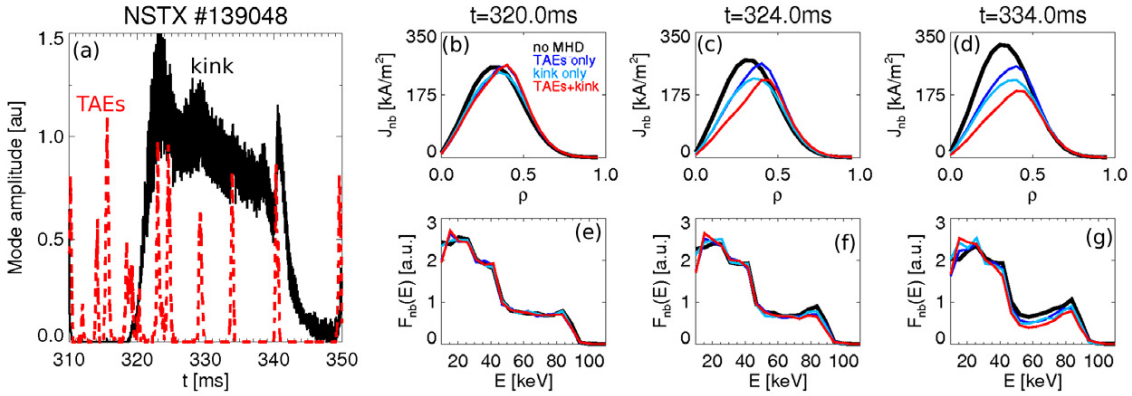


**Figure 7.** Modifications of NB-driven current by TAEs and kink-like modes. (*a*) Normalized mode amplitude evolution. (*b*)–(*d*) $J_{\rm nb}(\rho)$ at three different times assuming different instabilities acting on fast ions. Thick black profiles refer to the no-mode case. (*e*)–(*g*) Variations of the fast ion energy distribution around $\rho = 0.5$ for the cases in (*b*)–(*d*).

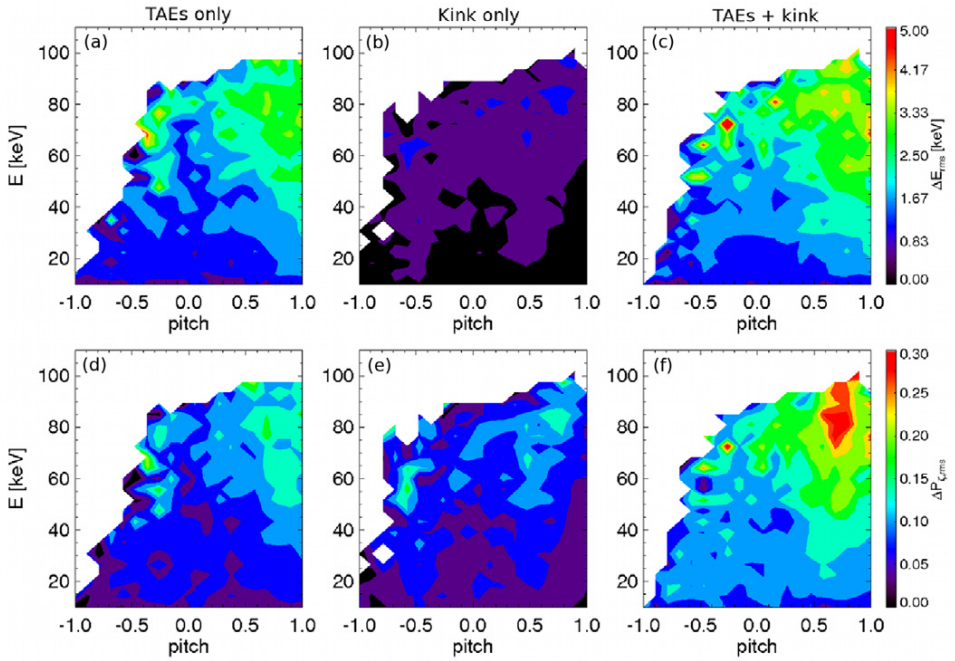


**Figure 8.** Detail of the phase space dependence of $E$ and $P_\zeta$ variations computed by the *kick* model for the cases show in figures 7(*c*)–(*f*). Variations are computed as the rms values $\Delta E_{\rm rms}$, $\Delta P_{\zeta,\rm rms}$ for the original fast ion distribution $F_{\rm nb}(E, p)$ around $\rho = 0.5$. (The variable *pitch* is defined as the ratio of parallel to total fast ion velocity.)

### *3.2. Full time-dependent analysis*

From the previous section, it may be concluded that simple diffusive/convective models may not be adequate to describe the detailed evolution of the fast ion distribution under the effects of instabilities. Long time scale simulations show that relevant differences are also found in more 'global' quantities, such as NB-CD efficiency and fast ion losses, which in principle might be expected to be more resilient to the details of the modeling.

Figure 9 shows the ratio of NB-driven current density as a function of time, computed using the ad-hoc $D_{\rm fi}$ and the 'kick' models. Results are normalized to the current density computed in the absence of any additional fast ion transport from instabilities (*classical* predictions). Unlike for the transient analysis, fast ion transport is here active for most of the discharge showing cumulative effects on the fast ion distribution that persist over several slowing down times. Overall, both transport models predict a comparable reduction in the central current $J_{\rm NB}$ and a redistribution to outer regions. The time evolution is however different. Because of the assumption of spatial uniformity of the $D_{\rm fi}(t)$ coefficient, the ad-hoc model predicts a relative variation whose radial profile does not depend strongly on time. Conversely, predictions from the 'kick' model show larger profile variations as time evolves, which is more consistent with the evolution of profiles (e.g. $q(r)$, magnetic equilibrium) and therefore of the topology of fast ion phase space over which instabilities are acting.

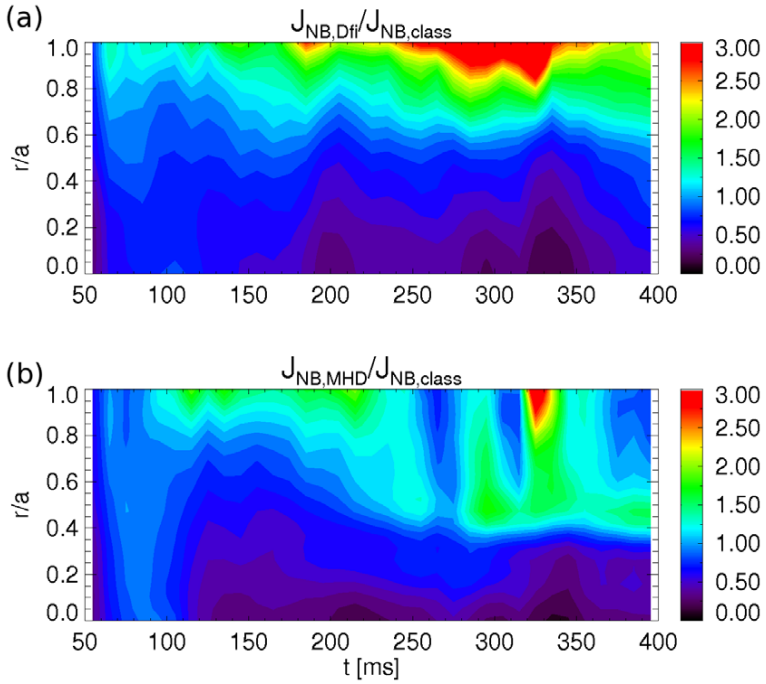


**Figure 9.** (*a*) Ratio of NB-driven current densities computed by TRANSP using enhanced diffusivity $D_{fi}(t)$ (cf figure 3(*b*)) with respect to classical predictions. (*b*) Same as (*a*) for current densities obtained using the new 'kick' model.

Differences clearly propagate when the *total* NB-driven current, $I_{NB}$, and the current deficit with respect to classical predictions are computed, see figure 10(*a*). For instance, a relatively minor deficit (average ≈20%) is found during the plasma current flat top, $t > 250$ ms, when the 'kick' model is used. Similarly, fast ion losses are much reduced (figure 10(*b*)), consistently with detailed analysis of the same discharge with the ORBIT code [5]. As a comparison, the average deficit computed with the ad-hoc $D_{fi}$ model is twice as large with respect to the 'kick' model, ≈40%. Fast ion losses are also enhanced, with spikes corresponding to the TAE avalanche events. This is inconsistent with previous modeling, which found limited losses and pointed to net fast ion energy reduction as the main culprit for the observed neutron rate drops [5].

Along with the neutron rate, another metric that is used to evaluate the agreement between experimental results and simulations with enhanced fast ion diffusivity is the plasma stored energy. Total stored energy is calculated from equilibrium reconstruction codes such as EFIT [20] and LRDFIT [21]. The main difference in the results shown herein is that EFIT reconstruction lacks constraints from measurements of the $q(r)$ profile, which are included in the LRDFIT analysis. (Note that effects on the thermal energy are not captured in these simulations, since experimental thermal profiles are used as input to the code).

The comparison between stored energy from EFIT/LRDFIT and from TRANSP simulations is shown in figure 10(*c*). Stored energy computed with the 'kick' model is lower than classical, as could be expected from a net fast ion energy loss caused by the instabilities, and within the range computed from equilibrium reconstruction. The total stored energy from TRANSP using the ad-hoc $D_{fi}$

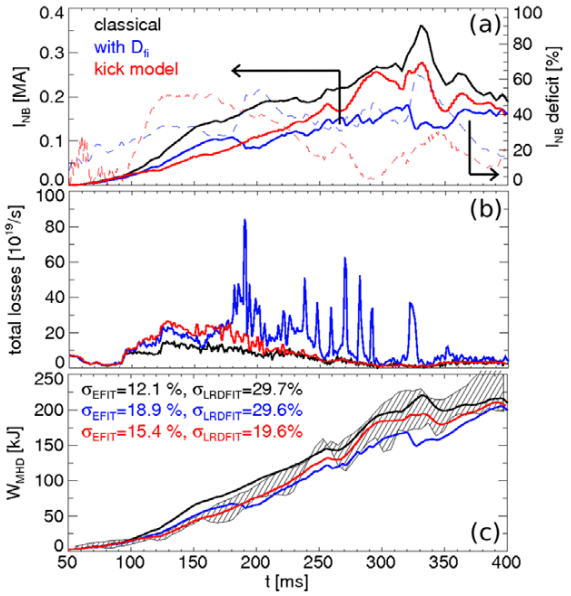


**Figure 10.** (*a*) Comparison of the total NB-driven current computed through TRANSP for the classical case, assuming an enhanced diffusivity $D_{fi}(t)$ and using the new 'kick' model (left axis, solid lines). Also shown is the computed deficit of the total NB-driven current for the two simulations with enhanced diffusivity and with the 'kick' model (right axis, dashed lines). (*b*) Fast ion losses for the three cases. (*c*) Total stored energy from classical, ad-hoc $D_{fi}$ and kick models. The shaded region represents the reference range of $W_{MHD}$ values obtained from EFIT and LRDFIT equilibrium reconstructions. The figure of merit $\sigma$ indicates the relative discrepancy of modeled *versus* measured $W_{MHD}$, averaged over $t \in (100, 400)$ ms.

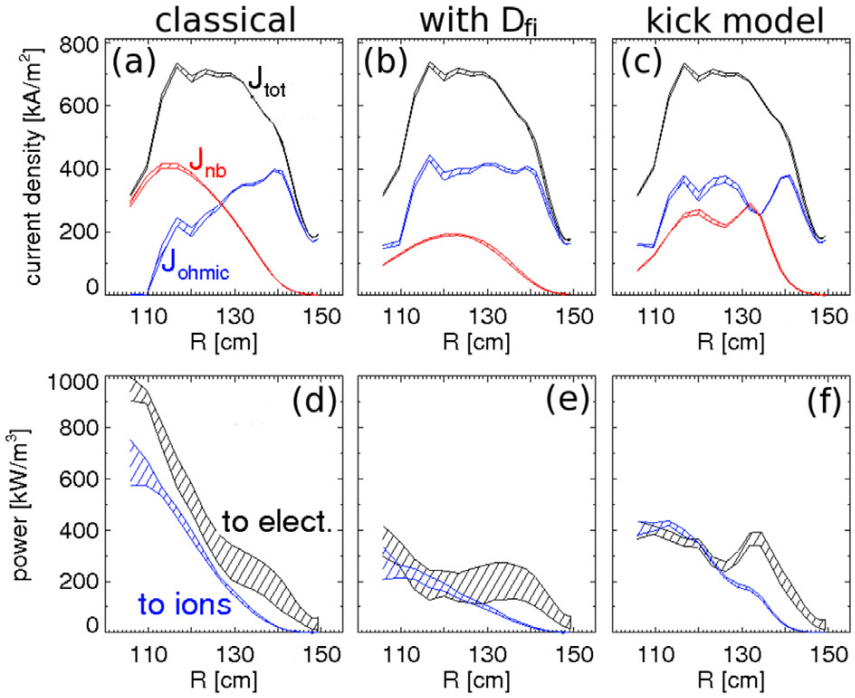


**Figure 11.** (*a*)–(*c*) Current density profiles calculated by TRANSP with different assumptions for fast ion transport (NSTX #139048). TRANSP results are averaged over $t = 300$–$305$ ms. (*d*)–(*f*) Total heating power transferred to electrons and ions for the three cases.

model is systematically lower than the reconstructed values. It is also lower than the values from the 'kick' model, consistently with the enhanced fast ion losses (figure 10(*b*)). Overall, results obtained with the 'kick' model are more consistent with the stored energy computed from LRDFIT (which is typically 5–20% lower than that calculated by EFIT). The average deviation between TRANSP and EFIT/LRDFIT stored energy is also shown in figure 10(*c*). Assuming that LRDFIT reconstructions are more accurate, since they include additional information on the measured $q(r)$ profile, it would be tempting to conclude that the 'kick' model provides a better match to both measured neutron rate *and* stored energy. However, more statistics from a larger number of cases is required to confirm this conclusion.

It should be emphasized that modifications of fast ion dynamics by instabilities are not relevant for fast ion physics and NB-driven current profile evolution only. For example, energetic particles represent a primary heat and momentum source for the thermal plasma. Simple models for fast ion transport are already used to assess global dependencies and trends when transport departs from classical. More quantitative estimates and predictions of local confinement, including *thermal* transport properties, must therefore include a consistent treatment of energetic particle physics, as pointed out in [13]. Although a complete analysis of thermal transport properties is beyond the scope of this work, a qualitative example is shown in figure 11, where the total power transferred to the thermal components is shown for different assumptions on fast ion transport. This power is the main source term entering in the ion and electron power balance equations, from which thermal conductivities are derived and through which confinement properties are inferred [22]. For a given profile of the *total* current density, resulting from the equilibrium reconstruction constrained by experimental data, an interplay between NB-driven and ohmic contributions is observed. (Bootstrap current is unchanged for the different cases). In practice, this implies that fast ion transport affects estimates of thermal transport in—at least—two ways: (i) directly, through the radial distribution of power density from slowing down fast ions; (ii) indirectly, through modification of the ohmic heating profile (and other quantities).

## 4. Summary and conclusions

The effects of MHD instabilities such as toroidal Alfvén eigenmodes and low-frequency kink-like modes on NB-CD have been investigated for a NB-heated NSTX plasma. Two approaches have been used in TRANSP simulations to compute the fast ion response to instabilities, hence the NB-driven current profile and its temporal evolution. The first approach mimics the effects of instabilities through an ad-hoc, spatially uniform diffusion coefficient, whose level is adjusted to match the measured neutron rate. The second approach utilizes a newly developed reduced model which takes into account the physics and constraints of wave–particle interaction.

Simulations indicate that instabilities can have a profound effect on NB-driven current. Moreover, it is found that simple diffusive models for fast ion transport may not be adequate to capture the correct evolution of the current profile. Selective modifications of fast ion phase space are indeed important. Simulation results for other quantities, such as the total (thermal plus fast ion) stored energy, also confirm the

importance of capturing fast ion phase space modifications by the instabilities.

An important conclusion of this work is that MHD effects on NB-driven current evolution are quite sensitive to the properties of the instabilities. Mode location, frequency and amplitude determine which portions of the fast ion distribution are affected, and these dependencies can not be properly taken into account by simple diffusive (or diffusive/convective) models. Mode properties must therefore be inferred from experiments or from physics-based models and codes for quantitative analysis and predictions. In addition, mode-induced transport must be modeled according to the correct physical mechanisms of wave–particle interaction. The new reduced model implemented in the TRANSP code addresses this latter issue. Future work will focus on extensive validation of the new model for a variety of scenarios, possibly across multiple devices. The overall goal is to assess the implications of fast ion phase space modifications by instabilities on integrated simulations. These effects are expected to be even more important for integrated modeling of burning plasmas (e.g. in ITER and DEMO), in which energetic particles from fusion reactions, RF heating and NB injection represent the dominant heat source.

## Acknowledgments

This material is based upon work supported by the US Department of Energy, Office of Science, Office of Fusion Energy Sciences under contract number DE-AC02-09CH11466.

## References

[1] Cheng C.Z. 1992 *Phys. Rep.* **211** 1
[2] Gorelenkov N.N., Cheng C.Z. and Fu G.Y. 1999 *Phys. Plasmas* **6** 2802
[3] Crocker N.A. *et al* 2011 *Plasma Phys. Control. Fusion* **53** 105001
[4] Fredrickson E.D. *et al* 2009 *Phys. Plasmas* **16** 122505
[5] Fredrickson E.D. *et al* 2013 *Nucl. Fusion* **53** 013006
[6] Mynick H.E. 1993 *Phys. Fluids* B **5** 1471
[7] Podestà M., Gorelenkova M. and White R.B. 2014 *Plasma Phys. Control. Fusion* **56** 055003
[8] Pankin A., McCune D., Andre R., Bateman G. and Kritz A. 2004 *Comput. Phys. Commun.* **159** 157
[9] Goldston R.J., McCune D.C., Towner H.H., Davis S.L., Hawryluk R.J. and Schmidt G.L. 1981 *J. Comput. Phys.* **43** 61
[10] Baranov Y.F., Jenkins I., Alper B., Challis C.D., Conroy S., Kiptily V., Ongena J., Popovichev S., Smeulders P., Surrey E., Zastrow K. and JET EFDA contributors 2009 *Plasma Phys. Control. Fusion* **51** 044004
[11] Gerhardt S.P. *et al* 2011 *Nucl. Fusion* **51** 033004
[12] Turnyanskiy M., Challis C.D., Akers R.J., Cecconello M., Keeling D.L., Kirk A., Lake R., Pinches S.D., Sangaroon S. and Wodniak I. 2013 *Nucl. Fusion* **53** 053016
[13] Heidbrink W.W. *et al* 2014 *Plasma Phys. Control. Fusion* **56** 095030
[14] Klimek I., Cecconello M., Gorelenkova M., Keeling D., Meakins A., Jones O., Akers R., Lupelli I., Turnyanskiy M., Ericsson G. and The MAST Team 2015 *Nucl. Fusion* **55** 023003
[15] Chen L., Vaclavik Y. and Hammett G.W. 1988 *Nucl. Fusion* **28** 389
[16] White R.B. 2014 *The Theory of Toroidally Confined Plasmas* 3rd edn (London: Imperial College Press)
[17] White R.B. 2012 *Commun. Nonlinear Sci. Numer. Simul.* **17** 2200
[18] White R.B., Gorelenkov N.N., Fredrickson E.D. and VanZeeland M.A. 2010 *Phys. Plasmas* **17** 056107
[19] White R.B. and Chance M.S. 1984 *Phys. Fluids* **27** 2455
[20] Lao L.L., John H.S., Stambaugh R.D., Kellman A.G. and Pfeiffer W. 1985 *Nucl. Fusion* **25** 1611
[21] Menard J.E. *et al* 2006 *Phys. Rev. Lett.* **97** 095002
[22] Hawryluk R. 1979 An empirical approach to tokamak transport (physics of plasmas close to thermonuclear conditions) *Proc. Int. School of Plasma Physics (Villa Monastero, Varenna, Italy, 1979)*